

Electric-Field-Induced Association of Colloidal Particles

Seth Fraden, Alan J. Hurd,^(a) and Robert B. Meyer

Martin Fisher School of Physics, Brandeis University, Waltham, Massachusetts 02254

(Received 15 May 1989)

Dilute suspensions of micron-diameter dielectric spheres confined to two dimensions are induced to aggregate linearly by application of an electric field. The growth of the average cluster size agrees well with the Smoluchowski equation, but the evolution of the measured cluster size distribution exhibits significant departures from theory at large times due to the formation of long linear clusters which effectively partition space into isolated one-dimensional strips.

PACS numbers: 64.60.Cn, 68.70.+w, 77.30.+d, 82.70.Dd

The study of irreversible aggregation of diffusing particles has been greatly elucidated by computer simulations, because graphic representation of the associating particles revealed the novel structures known as fractals. Experimentally, direct observation of diffusing aggregating particles has been restricted to particles confined to two dimensions.¹⁻³ Focusing a microscope on a colloidal suspension confined to a plane allows visualization of all the particles and permits measurement of statistical properties such as the evolution of the cluster size distribution. Additionally, the effect of the spatial distribution of clusters on the aggregation process can be assessed, and the observed motion of approaching particles and their subsequent bonding reveals further details of the aggregation process.

We present experimental studies of irreversible aggregation of micron-diameter polystyrene spheres suspended in an aqueous medium and confined to a thin layer, to which a high-frequency uniform electric field is applied in the plane of the sample. At high frequencies the spheres act as dielectric holes in the water. A single sphere distorts the field in such a way that it is equivalent to a dipole pointing along the external field. Once the spheres approach each other mutual polarization further distorts the field creating higher-order, although weaker, multipoles.^{4,5} The nonadditive nature of the field-induced multipoles and the alignment of the moments along the field direction distinguish this case from the previously studied system of spheres with permanent dipole moments.³

It is observed that a dilute suspension of dielectric spheres in a strong electric field will undergo linear aggregation forming clusters of spheres resembling pearl chains with the chain axis along the field.⁶⁻¹⁰ We present for this system the first measurements of the cluster size distribution of sufficient quality to quantitatively compare with the scaling predictions of irreversible aggregation.¹¹⁻¹⁴

Chain growth is a function of the amplitude of the field. When a large-amplitude field is applied, the spheres assemble into long chains. At high fields, association of the spheres is irreversible in the sense that clusters are never seen to break as long as the field is on.

The chains are flexible: Within one chain fluctuations in the sphere-sphere separation and in the angle between sphere centers and the external applied field are observed. When the field is turned off the chains break up, and the particles diffuse apart. The charge on the colloids creates a short-range repulsive potential that prevents van der Waals forces from permanently bonding the particles. High-resolution microscopy reveals that the sphere surfaces are separated by (5-10)% of a diameter at our highest applied field.

With low-amplitude fields the association of particles is reversible. Chains form and break apart into smaller chains, and after a transient period a dynamic equilibrium among clusters is reached with a time-independent cluster size distribution. At low field amplitude, the lifetime, mean size of the chains, and fluctuations within a chain are strong functions of the applied field strength. This process of reversible association will be discussed in a future publication.

A single uncharged dielectric sphere immersed in a solvent distorts a uniformly applied electric field in such a way that the field outside the sphere can be described as the superposition of the undistorted field and the field due to a point dipole located at the center of the sphere with moment

$$\boldsymbol{\mu} = \epsilon'_w a^3 \left[\frac{\epsilon_p - \epsilon_w}{\epsilon_p + 2\epsilon_w} \right] \mathbf{E}, \quad (1)$$

with ϵ_w, ϵ_p the complex dielectric constants of the solvent and the particle, where $\epsilon = \epsilon' + i\epsilon''$, a the radius of the sphere, and \mathbf{E} the electric field.^{4,6,15} Two spheres separated at large distances interact primarily through a dipole-dipole potential with the interaction energy given by

$$U = \frac{\mu^2}{8\epsilon'_w a^3} \frac{1 - 3\cos^2\theta}{(1 + \xi)^3}, \quad (2)$$

where θ is the angle between the line connecting the centers and the external field and the separation between sphere centers is $r = 2a(1 + \xi)$. When $\epsilon_w \gg \epsilon_p$, the ratio of the field energy to the thermal energy for two dipoles in contact is $U/kT = \epsilon'_w a^3 E^2 / 32k_B T$. Since polystyrene is charged in water, it is surrounded by a shell of coun-

terions. However, if the field alternates faster than the double layer can follow there will be no induced dipole moment in the double layer and only dielectric polarization of the polystyrene occurs. This cutoff frequency is approximately equal to the inverse of the time for the ions to diffuse the radius of the sphere, which for 1- μm spheres occurs between 1 and 10 kHz.¹⁶

The sample cell is composed of two glass microscope slides. Transparent, indium-tin-oxide electrodes were on one slide, etched by photolithography from precoated glass slides, thereby leaving conductive strips on the glass. A 477- μm gap between electrodes was employed in this study. The other slide consisted of a small rectangular piece of glass glued with optical cement to a microscope slide and was positioned above the electrode gap. Polystyrene spheres of 1.27 μm diam were suspended in a 50-50 mixture of D_2O and H_2O to match the density of the polystyrene. Potassium chloride was added to the suspension to increase the dielectric constant of the thin aqueous layer relative to the glass slides and thus to confine the electric field. The final salt concentration was 2 mM and a nonionic surfactant was added to promote stability of the suspension against salt-induced aggregation. Observations of the association of these particles were made directly with a microscope equipped with a video camera and a digital-image processor. A typical example of associating particles seen in the microscope is illustrated in Fig. 1.

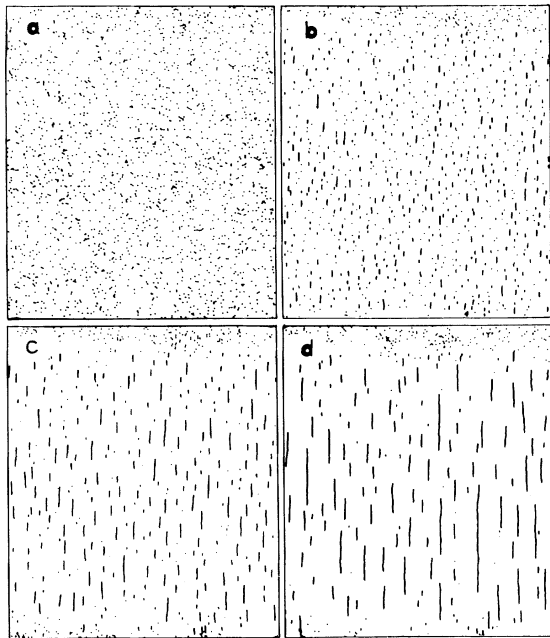


FIG. 1. Photographs of associating 1.27- μm balls. (a) No field, (b)–(d) 9.9, 66.7, and 210 sec, respectively, after turning on a 1000-V/cm ($U/kT=19$), 30-kHz electric field. The edges of the electrode, spaced 330 μm apart, are seen as regions where there are no chains.

The most frequently used theoretical description of irreversible aggregation is Smoluchowski's equation which describes the time evolution of the cluster size distribution. The rate of change of the population of clusters comprised of k monomers, $\dot{n}_k(t)$, is

$$\dot{n}_k = \frac{1}{2} \sum_{i+j=k} K_{ij} n_i n_j - \sum_{j=1}^{\infty} K_{kj} n_k n_j. \quad (3)$$

In the above equation, K_{ij} is the coagulation kernel and represents the probability per unit time for coalescence of an i cluster and a j cluster. Within this theory, the mechanism by which n_k changes with time is two clusters coagulating into a single larger cluster. The assumption that there are only binary collisions limits the applicability of the Smoluchowski equation to low cluster densities. Also, since there are no spatial variables in this equation, the Smoluchowski equation is necessarily of the mean-field form.

Computer simulations have shown that the cluster size distribution, $n_k(t)$, approaches a scaling form, $n_k(t) = M k^{-2} \phi(k/\bar{n}(t))$, and the Smoluchowski equation was also shown to support the same scaling form^{11–14} when the kernel is a homogeneous function of degree λ , i.e., $K(is, js) = s^\lambda K(i, j)$. The constant M is the total number of spheres, $M = \sum_k k n_k(t)$, and $\bar{n}(t)$ is the average length of the chains, $\bar{n}(t) = M/N$, where $N = \sum_k n_k(t)$. The simulations as well as analytical results have shown that $\bar{n}(t) \sim t^z$ for large times, where $z = 1/(1-\lambda)$. This relation holds for dilute systems undergoing linear aggregation even in two dimensions which appears to be the upper critical dimension.^{17,18}

To study irreversible aggregation we performed nine aggregation trials and the distributions were averaged together. The volume fraction for these runs was $\phi = 0.9\% \pm 0.04\%$, with $U/kT = 30.9 \pm 0.2$ at a frequency of 150 kHz. Typically 1000 spheres were in the field of view. At high fields the rate of aggregation was only slightly dependent on field strength in contrast to the low-field behavior.¹⁰ We can compare the measured rate of growth with the Smoluchowski equation. An argument was offered recently for the form of the kernel used to describe linear aggregation.¹⁷ The coagulation kernel K_{ij} is a product of an effective diameter of the cross section of two clusters, $R_i + R_j$, and a diffusion coefficient, $D_i + D_j$, where D_i and R_i are the diffusion constant and the radius of a cluster of size i , respectively. Since the chains aggregate by joining end to end, the cross section does not vary with chain length. The diffusion constant's dependence on chain length is assumed to be a power law or $D_i \sim i^\lambda$. Thus the coagulation kernel is given by

$$K_{ij} \sim i^\lambda + j^\lambda. \quad (4)$$

Measurement of the average chain length for the nine trials is shown in Fig. 2 from which we determined $z = 0.60 \pm 0.02$ and $\lambda = -0.67$. We assume that the friction coefficient of a chain of i spheres, η_i , scales like

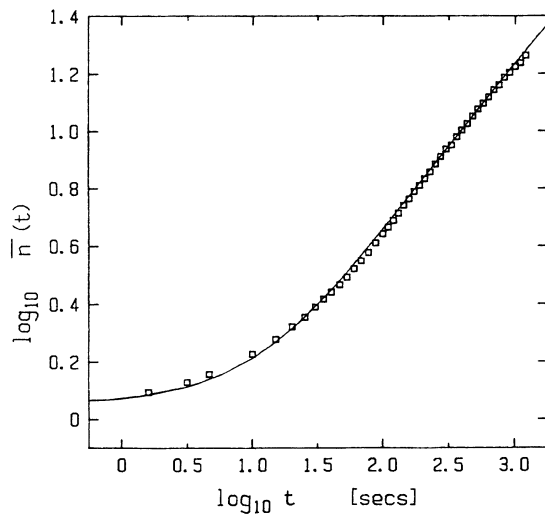


FIG. 2. Average chain length as a function of time for the Smoluchowski theory (—) and experiment (□). The volume fraction was $\phi=0.9\%$ and interaction strength $U/kT=30.9$. The exponent describing the growth of the average chain length ($z=0.60$) was determined during the time interval 100–1000 sec. One arbitrary constant was used to scale the units of time between the Smoluchowski equation and experiment.

$\eta_i \sim i^{-\lambda}$. In the absence of hydrodynamic coupling between spheres $\lambda = -1$. Actually a given sphere moves in the slip stream of its neighbors and η_i is significantly less than $i\eta_1$. Thus we expect that $\lambda > -1$ for chains of moderate length. We have kindly been given a computer program by Johnston¹⁹ that numerically integrates the Smoluchowski equation using a predictor-corrector technique.²⁰ Integration was terminated when 1% of the mass was present in clusters larger than 120. Using the kernel from Eq. (4) with $\lambda = -0.67$ and the experimentally measured initial distribution of cluster sizes, Eq. (3) was numerically solved to yield the cluster size distribution as a function of time, from which we extract the average length, also shown in Fig. 2.

The experimental cluster size distributions are shown in Fig. 3 at different stages of aggregation. As time progresses the distribution broadens, but there are always some of the small-sized clusters present. Viewed under a microscope the motion of a cluster appears diffusive until two clusters are about a particle diameter away from each other. Then the ensuing motion is ballistic and, for example, a monomer adding onto a long chain snaps into position at the end of a chain. The larger chains diffuse more slowly than the smaller chains, but with time clusters continue to coalesce into longer and longer chains. At later stages of aggregation there are often small clusters, such as monomers or dimers, diffusing between two long chains. These small clusters must migrate to the end of a chain before they can aggregate, which can take a long time. Thus long

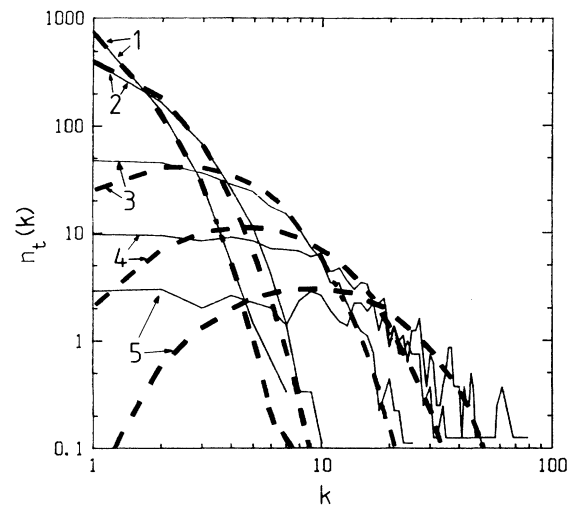


FIG. 3. The evolution of the cluster size distribution measured at different times after application of the field: (1) 1.6, (2) 10, (3) 100, (4) 330, and (5) 1000 sec. Measured distributions: —. Distributions calculated from the Smoluchowski theory using the kernel extracted from the growth of the average chain length: ····.

chains effectively cut the plane into strips and we observe the beginnings of crossover from two- to one-dimensional behavior.¹⁷ This is the first experimental observation of this effect. Occasionally it was observed that spheres stuck temporarily to the glass. This would prevent the monomer peak from disappearing, and could hamper the decay of those small clusters that contained one anchored particle. However, watching videotapes of the experiments showed that at least half of the small clusters during the late stages of aggregation were freely diffusing. In Fig. 3 the experimental distributions as a function of time are compared with the theoretical cluster size distribution generated by the numerical solution of the Smoluchowski equation using the experimentally observed initial cluster size distribution. The predicted decrease of the number of small clusters at large times is strikingly different from the experiment. Figure 1(d) is a typical example of the spatial distribution of chains at the beginning of crossover. A long chain prevents chains on opposite sides from diffusing perpendicular to the chain axis and coalescing but eventually the chains on the sides can diffuse around the end of the long chain since all chains are of finite length. Thus strictly one-dimensional aggregation is never observed in the time course of the experiment. Indeed, a recent theoretical study¹⁸ predicts that for the kernel of Eq. (4) the crossover time is infinity.

The scaling form of $n_k(t)$ discussed above suggests that a plot of $k^2 n_k(t)/M$ vs $k/\bar{n}(t)$ for all distributions at all times should fall on a single curve, as shown in Fig. 4(a). The entire aggregation run is plotted in this figure, from 0.03 to 1000 sec after the field was turned on.

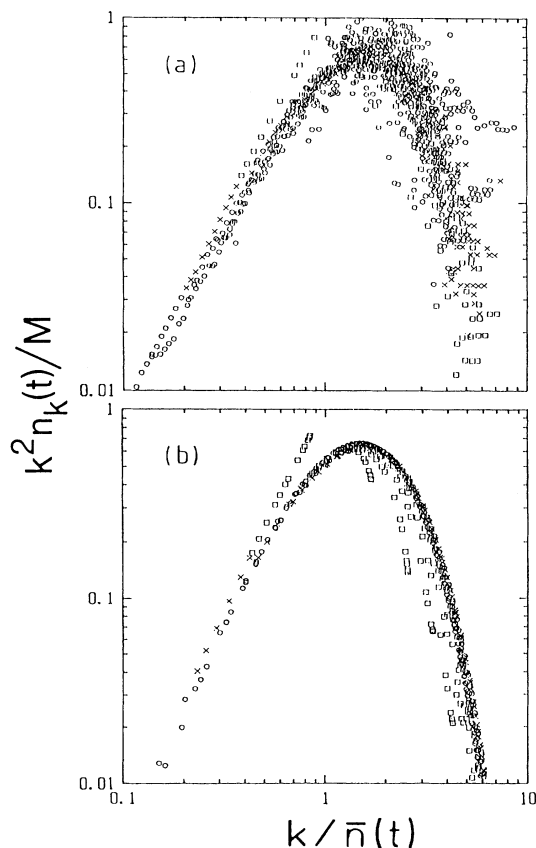


FIG. 4. Scaling form of the cluster size distributions shown in Fig. 3. Over forty cluster size distributions spanning times from 0.1 to 1000 sec are plotted here. At early times, when $\bar{n}(t) < 2.5$ ($t < 35$ sec), the cluster size distribution does not scale. \square , $0 < t < 35$ sec; \times , $35 < t < 120$ sec; and \circ , $120 < t < 1200$ sec. (a) Experiments. (b) Smoluchowski equation.

Scaling does not begin until after the average length is greater than about 2.5 diam. The early-time points are denoted by squares in Fig. 4(a). Note that the squares begin above the main body of points and come diagonally down to meet the curve as $k/\bar{n}(t)$ decreases. The squares for $k/\bar{n}(t) < 1$ represent the monomers of early distributions. A similar plot, generated from a numerical solution of Eq. (3), is shown in Fig. 4(b). It shows the same behavior as the experimental data: Only at later times does the distribution function scale.

In summary, we have measured the kinetics of irreversible association of diffusing colloids interacting with an induced dipole potential and compared the evolution of the cluster size distribution with the Smoluchowski

theory. The experimental distributions are similar to the Smoluchowski distributions except that there are always more small clusters observed experimentally than theoretically predicted. We suggest that this is a consequence of the two-dimensional nature of the sample, in which the long clusters effectively partition the space between them, isolating smaller clusters.

The research was supported by DOE Grant No. DE-FG02-87ER45084 and NSF Grant No. DMR-8803582 awarded to R.B.M. We would like to thank Dr. Z. B. Djordjevic for pointing out the relevance of the scaling arguments to this experiment.

(a)Current address: Division 1121, Sandia National Laboratories, Albuquerque, NM 87185.

¹A. Hurd and D. Schaefer, Phys. Rev. Lett. **54**, 1043 (1985).

²A. J. Armstrong, R. C. Mockler, and W. J. O'Sullivan, J. Phys. A **19**, L123 (1986).

³G. Helgesen, A. T. Skjeltorp, P. M. Mors, R. Botet, and R. Jullien, Phys. Rev. Lett. **61**, 1736 (1988).

⁴F. A. Sauer, in *Interactions between Electromagnetic Fields and Cells*, edited by A. Chiabrera, C. Nicolini, and H. P. Schwan, NATO Advanced Study Institutes, Ser. A, Vol. 97 (Plenum, New York, 1985), p. 181.

⁵D. J. Jeffrey, Proc. Roy. Soc. London A **335**, 355 (1973).

⁶L. D. Sher, Ph.D. thesis, University of Pennsylvania, 1963 (unpublished).

⁷H. P. Schwan, in Ref. 4, p. 371.

⁸S. Takashima and H. P. Schwan, Biophys. J. **47**, 513 (1985).

⁹L. D. Sher, E. Kresch, and H. P. Schwan, Biophys. J. **10**, 970 (1970).

¹⁰T. A. Vorob'eva, I. N. Vlodavets, and P. I. Zubov, Colloid J. U.S.S.R. **31**, 668 (1969).

¹¹T. Vicsek and F. Family, Phys. Rev. Lett. **52**, 1669 (1984).

¹²Z. B. Djordjevic, Ph.D. thesis, Massachusetts Institute of Technology, 1984 (unpublished).

¹³M. Kolb, Phys. Rev. Lett. **53**, 1653 (1984).

¹⁴P. G. J. van Dongen and M. H. Ernst, Phys. Rev. Lett. **54**, 1396 (1985).

¹⁵H. A. Pohl, *Dielectrophoresis* (Cambridge Univ. Press, London, 1978).

¹⁶K.-H. Lim and E. I. Franses, J. Colloid Interface Sci. **110**, 201 (1986).

¹⁷S. Miyazima, P. Meakin, and F. Family, Phys. Rev. A **36**, 1421 (1987).

¹⁸P. G. J. van Dongen, Phys. Rev. Lett. **63**, 1281 (1989).

¹⁹D. F. Johnston, Ph.D. thesis, Massachusetts Institute of Technology, 1983 (unpublished).

²⁰F. S. Acton, *Numerical Methods That Work* (Harper & Row, New York, 1970), pp. 130-146.